International Journal of Materials Science
ISSN 0973-4589 Volume 12, Number 2 (2017), pp. 239-258

http://www.ripublication.com

Effect of Resistive Coupled Microwave Sintering on the Micro Hardness and Thermal Properties of Infrared Transparent Nano Yttria

Mathew C T, Jijimon K Thomas*, Swapna Y V, Jacob Koshy and Sam Solomon

Electronic Materials Research Laboratory, Department of Physics,
Mar Ivanios College, Thiruvananthapuram 695015, Kerala, India.
**Corresponding author*

Abstract

Resistive coupled microwave sintering technique which couples the resistive heating and microwave heating effectively is employed to sinter infrared transparent yttria to 99.2% of the theoretical density. The pellets fabricated from the ultra-fine nano powder with average particle size ~15nm synthesized by combustion technique and sintered at 1450^{o}C with an average grain size of 0.22μm. For a comparative study of the hardness and thermal properties two other variants of sintering strategies, conventional sintering and susceptor assisted microwave sintering are also employed. A comprehensive analysis on the hardness reveals that the hardness of the pellets sintered via resistive coupled microwave heating is 8.85 GPa and is superior to the pellets sintered using the other two techniques. The microhardness of the pellets sintered via resistive heating is found to be 6.64 GPa and that for pellets sintered via susceptor assisted microwave heating is 7.88 GPa. The thermal properties of the pellets like thermal conductivity, thermal diffusivity and the specific heat capacity are also analyzed in detail. The results clearly indicate that the yttria ultra fine nanophase powder synthesised by the single step combustion method and sintered via resistive coupled microwave heating shows better mechanical and thermal properties which can be used very effectively for the fabrication of infrared transparent windows and domes.

Keywords: micro hardness; resistive coupled microwave sintering; thermal diffusivity

1. INTRODUCTION

Infrared transparent windows found to have numerous applications like Infrared windows in homing missiles, infrared inspection ports, infrared cameras, laser technology, lamp envelopes, transparent armours, space craft windows and modern target acquisition systems[1-7].Yttria is one of the most intensively studied infrared transparent ceramics due to its excellent properties required for infrared transparent ceramics like, isotropic body centred cubic structure which is stable even at 1800^{o}C [8], moderate refractive index and absence of birefringence[1], high thermal conductivity and low thermal expansion coefficient[9], high thermal shock resistance [10], high melting point [11], moderate hardness [9,12], low emissivity in the mid infrared range at elevated temperatures [13] and high transparency in the visible and infrared range [14].

In addition to the transparent nature an infrared transparent window should protect the highly delicate infrared sensor from the harsh environments of missile flight. In the case of windows fabricated using polycrystalline powders, there is always a trade-off between infrared transparency and mechanical strength [15]. Grain size of the sintered pellet is one of the deciding factor of performance of an infrared transparent window. High temperature sintering above 1600^{o}C is required in the case of high quality transparent yttria. High temperature sintering and long soaking duration accelerates the grain growth and consequently the mechanical properties deteriorates [16]. It is observed that the fine grained materials show low diffuse transmission and high in-line transmission [17]. As the model suggested by Apetz and Bruggen [18] the transmittance through a sintered sample is highly dependent on the grain size. If the grain size is very small compared to the wavelength in consideration translucent materials becomes transparent even though there are multiple phases or phases other than cubic structure [19]. The sintering of yttria to its full density at lower temperature hindering the grain growth without compromising mechanical strength as well as the percentage of transmittance in the infrared range is the major challenge in the fabrication of infrared windows. Most of the materials with grain sizes in the nanometer regime exhibit significantly higher values of micro hardness compared to their coarse grained counterparts [20]. Even though the hardness of the window plays a crucial role in the performance of the infrared transparent window the research work on the hardness properties are relatively low. Recently it is reported that spark plasma sintering is effectively used to sinter yttria to 99.6% of the theoretical density at 1500^{o}C with average grain size 0.58μm which showed a transmittance of 80% in the mid IR range and 66% at 800nm and the hardness reported is 7 GPa [21]. In earlier reports conventional sintering yielded pellets having 99.4% of the theoretical density with an average grain size of 21.5 μm with a transmittance of 60% at 1000 nm and a hardness of 7.5GPa [22]. Serivalsatit et al were able to sinter Er doped yttria by a two step sintering process to 99.73% of the theoretical density with an average grain size of 0.328μm which showed a transmittance of 38% at 2000 nm and a hardness 7.23 GPa. After the application of hot isostatic pressing the transmittance improved to 75% at 800nm and the hardness improved to 9.09GPa [9]. In all the above cases either a sintering additive is used or hot isostatic pressing is employed. A large quantum of

works are reported so far in reducing the sintering temperature and enhancing the transmittance properties[23-30], but no comprehensive analysis in improving the transmittance properties without compromising the mechanical properties in pellets sintered using the resistive coupled microwave sintering technique is reported in the literature to the best of our knowledge.

During the missile flight there is a possibility to have a considerable temperature difference between the outer and inner surfaces of the window. If the window material is unable to tolerate this thermal stress it will shatter. Resistance to thermal failure by thermal shock is a critical requirement for some applications . Ideally domes and windows should be made as thin as necessary to withstand aerodynamic pressures to obtain the maximum thermal shock resistance [31]. To achieve high thermal shock resistance figure of merit to prevent the shattering the window material during the missile flight, it should possess high thermal conductivity. Ideally the thermal conductivity values should be in the range 7-50 $Wm^{-1}K^{-1}$ [32]. Even though the thermal conductivity is playing a vital role in the performance of high quality transparent window no much work are reported in the literature regarding this.

Due to the increasing need of infrared transparent windows in various applications a large quantum of research is happening in this filed for the last few decades. The most recent works are focussing on improving the properties of the currently available materials along with the search of new materials which can be effectively used as infrared transparent windows. In the present work, a single step modified combustion method developed by us[33] has been used as an effective technique for the synthesis of phase pure nanoparticles of yttria ceramic of particle size (5-20 nm). The powder is further compacted to an optimum density at a much lower temperature with reduced grain size and good transparency to infrared radiation using resistive coupled microwave heating technique. As a key focus of this work the hardness properties of the samples sintered via conventional resistive heating, susceptor assisted microwave heating and resistive coupled microwave heating are compared to establish the effectiveness of resistive coupled microwave sintering in the fabrication of infrared transparent windows. The thermal properties of the samples sintered via three variants of heating are also evaluated in detail.

2. EXPERIMENTAL PROCEDURE

In the present work a single step auto-igniting combustion method is used to synthesize nano structured yttria [34]. Stoichiometric amount of high purity $Y(NO_3)_3.6H_2O$ (99.99%, Alfa Aesar, USA) is dissolved in double distilled water to make a clear solution. The amount of citric acid which is acting both as the fuel and complexing agent is calculated considering the total valance of the oxidising and reducing agents and is added to the clear solution which ensures maximum release of energy during combustion [35]. The oxidant to fuel ratio of the system is adjusted by adding nitric acid and ammonium hydroxide. The pH of the precursor mixture is adjusted to ~7. Here the nitric acid is acting as an oxidising agent which reacts with ammonium hydroxide to form ammonium nitrate. The so formed ammonium nitrate

acts as an extra oxidant without changing the proportion of the other reactants of the chemical reaction. Ammonium nitrate produces an increase in combustion gas consequently increases the surface area of the produced powder resulting fine quality nano powder. The solution containing the precursor mixture was heated using a hot plate at 250 ^{o}C in a ventilated fume hood. The solution boils on heating and undergoes dehydration accompanied by foam. The foam then ignites by itself on persistent heating giving voluminous and fluffy product of combustion.

The as-prepared samples are characterized by X-ray diffractometer (X'pert pro, PANalytical, the Netherlands) with Cu Kα radiation in the range of 20–60^{o} in steps of 0.0840 for the determination of crystalline structure and phase of the nanomaterials. The average crystallite size is estimated for all the samples from Scherrer's equation. The as prepared powder is uniaxially compacted in to pellets in a 14 mm diameter steel die at 20 MPa using a hydraulic press . The sintering of the disc shaped pellets are carried out in a high temperature furnace with molybdenum heating elements (TE-4050,Therelek, India) which employs the resistive heating. Sintering of the pellets are also carried out using susceptor assisted microwave furnace (VBCC/MF/86, VB Ceramics Consultants, India). The microwave heating is realized using a pair of 2.45 GHz magnetrons with power 1.1KW each. The temperature controller is able to maintain a temperature within the chamber with a maximum error limit of $\pm 1^{o}C$. The maximum possible error in estimating the temperature by the pyrometer is given as $\pm 10^{o}C$.A resistive coupled microwave furnace with a pair of molybdenum disilicide heating elements (VBCC/HMF/71,VB Ceramics Consultants, India) is also used for sintering the samples by effectively coupling the resistive and microwave heating. The experimental density of the sintered pellets is calculated using Archimedes principle. The surface morphological study of the sintered pellets are performed in a scanning electron microscope (NOVA NANOSEM-450, FEI, USA). Thermal conductivity and diffusivity of the samples are measured and compared using nano flash thermal conductivity meter (LFA 447, NETZSCH, Germany). The hardness of the sintered samples are tested using Vickers indenter method (HMV 2TAW, Shimadzu, Japan).

3. RESULTS AND DISCUSSION

The XRD patterns of as prepared Y_2O_3 nano powder is shown in figure 1. The X-ray diffraction analysis confirms the formation of single-phase cubic yttria nanoparticles without carrying out post annealing or calcination process. All the peaks are indexed for a cubic structure with mean lattice parameter a=10.58 Å which agree well with the XRD data reported of 10.60 Å in JCPDS file no.89-5591. The crystallite size calculated using Scherrer formula [36] for the major (*222*) peak is found to be 14.4 nm and the interplanar spacing corresponding to the plane is 0.3060 nm which matches very well with the value 0.3062 nm in the JCPDS reference. The crystallite size calculated from the XRD peaks lie in the size range 5-20 nm with an average particle size of 15 nm.

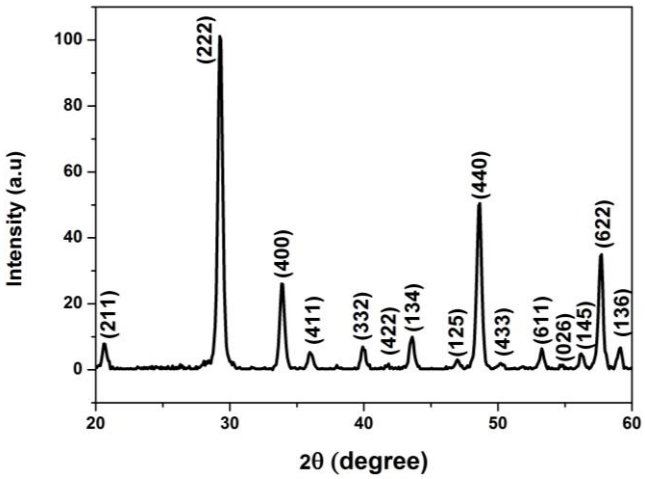

Figure.1: XRD pattern of as prepared nano yttria

The phase pure yttria powder is uniaxially compacted in to pellets in a 14 mm diameter steel die at 20 MPa using a hydraulic press. To study the sintering behaviour of the sample different sintering techniques are used and an effective comparison among the sintering processes which employ resistive heating, susceptor assisted microwave heating and resistive coupled microwave heating. For effective comparison of the sintering techniques and to optimise the sintering strategy a number of green pellets with same pressing conditions are used in the sintering process. For ease of discussion the pellet sintered via resistive heating, susceptor assisted microwave heating and resistive coupled microwave heating are coded as Y_R, Y_{SM} and Y_{RM} respectively.

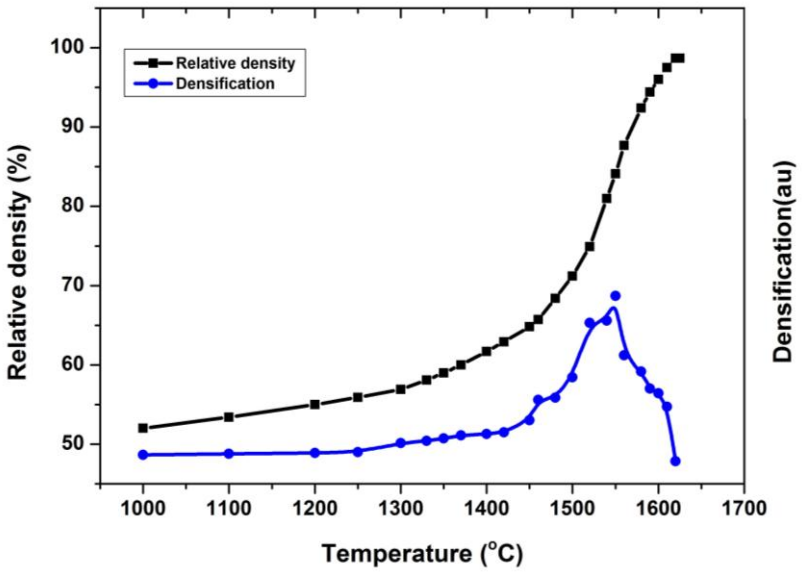

Figure 2: Variation in relative density and densification of the sample with sintering temperature during conventional sintering.

Initially the compacted pellet is placed in a conventional furnace which employs resistive heating. A uniform heating rate of $10^{o}Cmin^{-1}$ is used for the process. During the trial and error approach it is observed that a heating rate below this the grain size become large and a rate above this produce some cracks in the pellet. Figure 2 shows the variation in relative density and the densification with temperature. In conventional sintering it is found that the variation in relative density with temperature is very small up to $1300^{o}C$ after which the densification gradually increases and peaks around $1550^{o}C$. The pellet is sintered to 98.7% of theoretical density by holding for two hours at $1620^{o}C$. In susceptor assisted microwave sintering the pellet is placed in the microwave chamber in a silicon carbide susceptor and a heating rate of $40^{o}Cmin^{-1}$ is used for sintering the sample. The result is amazing that the pellet achieved a density of 98.9% of the theoretical density at $1540^{o}C$ for a soaking duration of just 20 minutes. In addition to the microwave energy the pellet is absorbing heat from the silicon carbide susceptor in which the pellet is placed which helps to couple the microwave energy effectively in a low loss material like yttria. The densification analysis shown in figure 3 reveals that in microwave sintering the densification triggers around $1300^{o}C$ and peaks around $1450^{o}C$ which is $100^{o}C$ lower than that observed in conventional sintering.

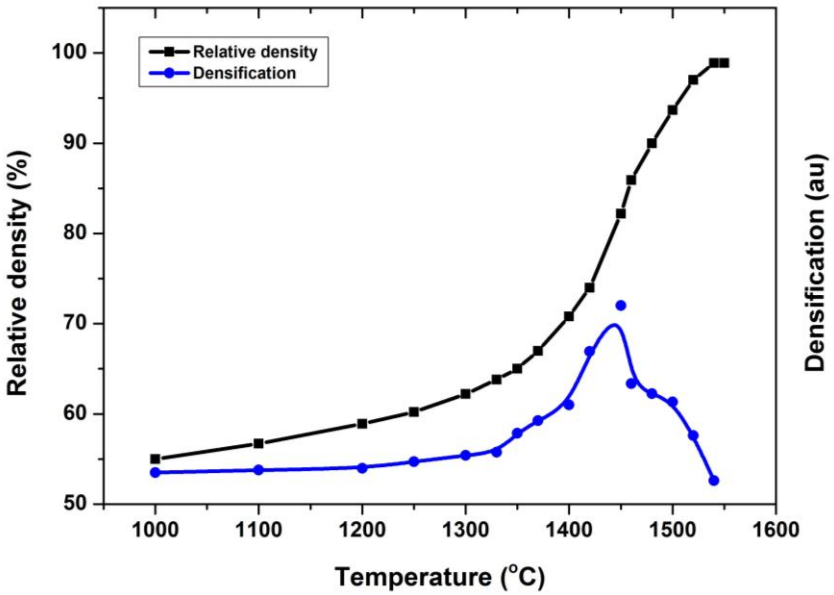

Figure 3: Variation in relative density and densification of the sample with sintering temperature during susceptor assisted microwave sintering.

A sintering strategy by coupling different proportions of microwave heating and resistive heating is also utilised to sinter infrared transparent yttria. In a resistive coupled microwave furnace, the pellets kept in the chamber are heated at a constant rate of $40^{o}Cmin^{-1}$. The maximum sintered density is obtained for the pellet sintered by coupling the resistive and microwave heating in the ratio 60:40 respectively up to $1100^{o}C$ and in the ratio 40:60 thereafter. The pellet is sintered to 99.2% of the

theoretical density at a much lower temperature of 1450^{o}C at a soaking duration of 20 minutes. It is found that the sintering temperature is reduced considerably in resistive coupled microwave heating. From the figure 4 it is clear that the densification triggers around 1200^{o}C and peaks around 1348^{o}C. The substantial reduction in sintering temperature and fast densification at a comparatively low temperature yield highly sintered pellets with reduced grain size. In this technique the sample pellet is simultaneously attaining heat from the microwave generated by the magnetrons and molybdenum heating elements, which enhances the densification to a great extent. Resistive coupled microwave sintering is thus found to be a promising sintering method, effectively promoting the densification of yttria at lower temperature.

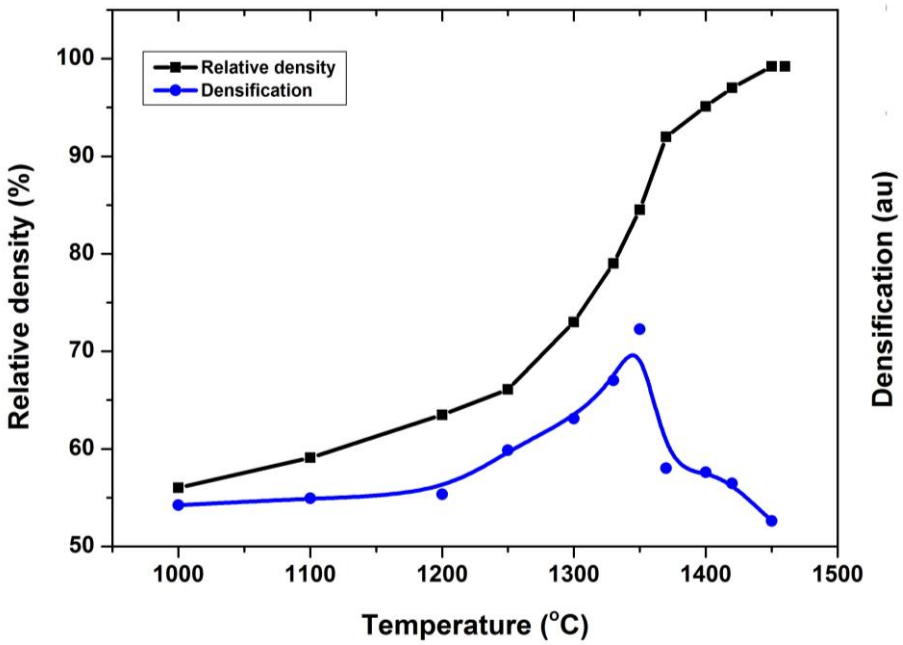

Figure 4: Variation in relative density and densification rate of the sample with sintering temperature during resistive coupled microwave sintering .

The well sintered pellets are hand polished and thermally etched at 1300^{o}C1550℃ for an hour in air in order to study the surface morphology of the sintered samples using Scanning Electron Microscopy. Figure 5(a) shows the SEM micrograph of the yttria ceramics sintered to 98.7% of the theoretical density. From the figure it is evident that the pellet is well sintered with minimum porosity. The grains are distinct confined with clear grain boundaries. The micrograph analysis reveals that that the grain are in the size range 0.2-2.1µm. The grain size distribution curve shown in figure 5(b) indicates that the maximum number of grains fall with in the size range 0.6 to 0.9 µm and the average grain size of the entire distribution is 0.72 µm.

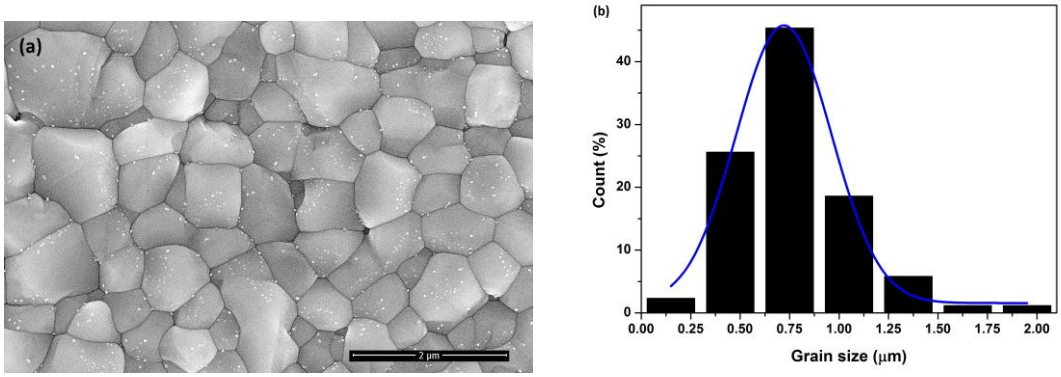

(a) **(b)**

Figure 5: (a) SEM micrograph of Y_2O_3 pellet sintered by resistive heating and **(b)** Grain size distribution of Y_2O_3 pellet sintered to 98.7% of theoretical density

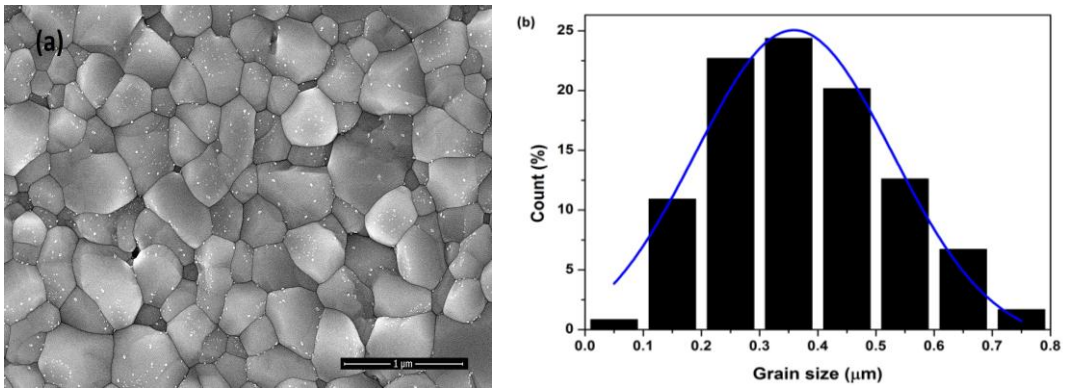

(a) **(b)**

Figure 6: (a) SEM micrograph of susceptor assisted microwave sintered Y_2O_3 pellet and **(b)** Grain size distribution of Y_2O_3 pellet sintered to 98.9% of theoretical density

Figure 6(a) shows the SEM micrograph of the susceptor assisted microwave sintered Y_2O_3 pellet. From the micrograph it is clear that size distribution of the grains are very small compared to that of conventionally sintered pellet. The microwave sintered pellets showed 98.9% of the theoretical density. The grain size distribution curve is shown in Figure 6(b). The graph clearly shows that the maximum numbers of grains are in the 0.2 to 0.4μm range and the average grain size of the entire distribution is 0.36μm.

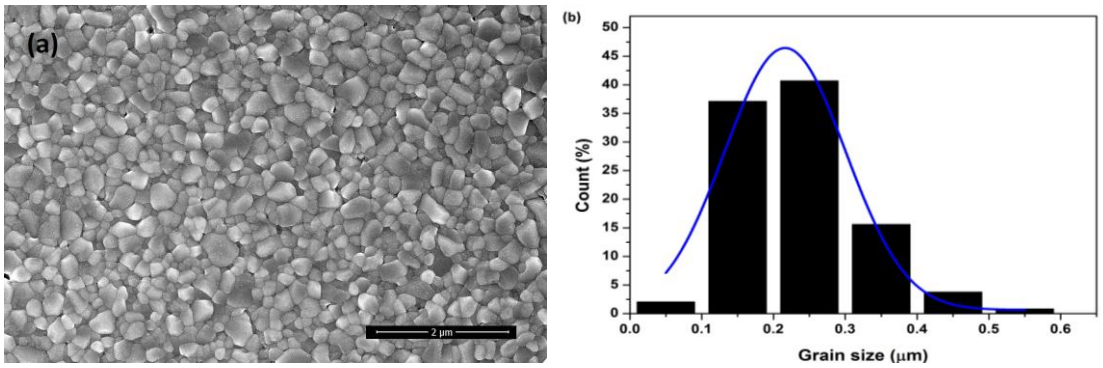

(a) **(b)**

Figure 7: (a) SEM micrograph of Y_2O_3 pellet sintered using resistive coupled microwave heating and **(b)** Grain size distribution of Y_2O_3 pellet sintered to 99.2% of theoretical density.

SEM micrograph of the Y_2O_3 pellet sintered to an optimum sintering density of 99.2% of theoretical density using resistive coupled microwave furnace is shown in Figure 7(a). From the micrograph it is clear that the pellet is well sintered with minimum pores and the full grown grains are in the size range of 0.025-0.7µm. Figure 7(b) shows the grain size distribution in Y_2O_3 pellet, from which it is evident that the maximum number of grains lie in the 0.2 to 0.3µm range and the average grain size of the entire distribution is as low as 0.22µm and it is the smallest of its kind reported so far in literature. Resistive coupled microwave sintering not only densify the sample, but also restricting any grain growth resulting the sample with finer microstructure compared to those sintered in resistive heating as well as microwave furnace. The actual driving mechanism and the sintering kinetics are not well established in the case of microwave sintering. There is a considerable change in activation energy in microwave sintering which indicates that the diffusion mechanism involved in the microwave sintering process is different from the conventional sintering which utilises the resistive heating mechanism [37]. Grain boundary diffusion in microwave sintering is triggered at a lower temperature in microwave sintering and plays a significant role in the sintering mechanism and at high temperature the grain boundary diffusion and volume diffusion coexist where as in conventional sintering volume diffusion plays vital role in the densification process [38].A large number of theories [39] are framed to unravel the mystery behind the so called microwave effect. The ponderomotive force induced by the electromagnetic field analogue to that in plasma physics may be the reason behind the enhanced sinterability and reduced grain size [40]. The slowly varying influence of a spatially nonuniform, high frequency electromagnetic field acting on a particle is referred to as a ponderomotive force. A high frequency harmonic electric field drives a high frequency flux of charge mobile species with in the medium. Even though the fluxes in the bulk of the medium are spatially uniform, the discontinuity of the medium near the surface results in a harmonic oscillation of the ionic concentration which are in phase with the high

frequency electric field oscillations which in turn produce a rectified quasistaionary flux of charge carriers. If the mobility of charge carriers in the near surface layer is greater than that in the bulk, then the action of tangential component of high frequency electric field can result in much more intense mass transport. The stress developed by ponderomotive forces are of magnitudes similar to that developed during hot pressing which enhances the mass transport to a greater extent. The microwave induced current is directly proportional to the microwave power . In conventional plasma the ponderomotive transport is typically due to the gradients in the radiation field intensity, but in solid-plasma version the mass transport is due to the gradients in charge mobility [39, 40]. In both the susceptor assisted microwave sintering and resistive coupled microwave sintering the effect of ponderomotive force is evident, but the only difference is that in susceptor assisted microwave sintering a major part of the microwave power is absorbed by the susceptor and we have no control over the conventional sintering part. Where as in the case of resistive coupled microwave sintering the resistive power and microwave power can be varied according to the processing conditions and nature of the samples.

The thermal diffusivity of the sample pellets sintered via resistive heating, microwave heating and resistive heating are measured and analysed in detail. Figure 8 shows the thermal diffusivity of the samples Y_R, Y_{SM} and Y_{RM} at different temperatures. It is observed that diffusivity is decreasing with increase in temperature. The thermal diffusivity values of the samples Y_R, Y_{SM} and Y_{RM} are 5.69×10^{-6}, 5.53×10^{-6} and $5.42\times10^{-6} m^2 s^{-1}$ respectively at 303K where as the values reduces to 2.68×10^{-6}, 2.56×10^{-6} and $2.55\times10^{-6} m^2 s^{-1}$ respectively at 570K. The diffusivity is maximum for the pellet Y_R. For Y_{SM} and Y_{RM} the diffusivity is found to be low. In the case of The deterioration of diffusivity attributes to the reduced grain size which accelerate phonon scattering at the grain boundaries.

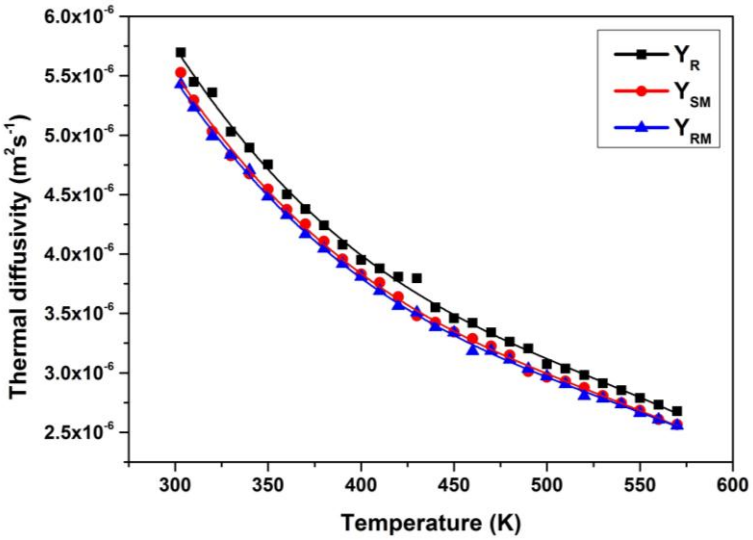

Figure 8: Thermal diffusivity of yttria pellets fabricated using different sintering techniques

The thermal conductivity of the sample pellets sintered via resistive heating , susceptor assisted microwave heating and resistive coupled microwave heating at different temperatures and their least squares fit to the data are as shown in the figure 9. The thermal conductivities of the samples at 300K are 13.06, 12.79 and 12.63 $Wm^{-1}K^{-1}$ respectively. The thermal conductivity of poly crystalline oxides decreases as temperature increases [42,43]. It is observed that in the case of resistive coupled microwave sintered pellet the thermal conductivity is slightly less than that in microwave processed and normal heat processed pellets. This is attributed to the reduced grain size , ie as grain size decreases phonon scattering increases and consequently conductivity decreases[44]. Even for the restively heated pellet with comparatively large grain size the thermal conductivity is less than the reported value of 13.5 $Wm^{-1}K^{-1}$ [1]. This may be due to the tiny pores present in the sample [45]. The gases trapped in the minute pores may adversely affect the thermal conductivity [46]. The experimental data agree very well with the reported values[47]. The reduction in thermal diffusivity and thermal conductivity will deteriorate the performance of the infrared transparent window. But it is important to note that there is no substantial reduction in thermal diffusivity and conductivity compared to the theoretical values and the values are in the range ideally suggested for infrared transparent windows [32].

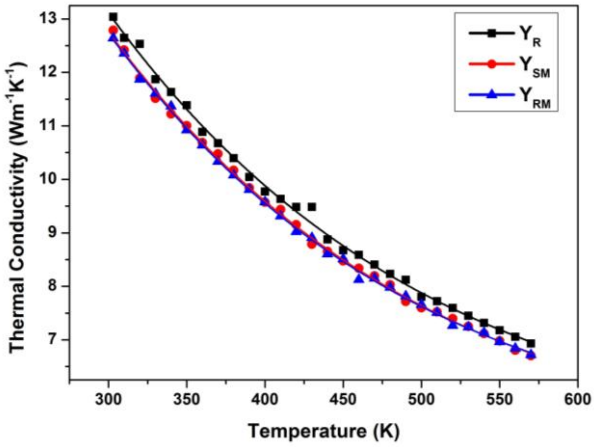

Figure 9: Thermal conductivity of yttria pellets fabricated using different sintering techniques

The variation in specific heat capacity with temperature is shown in Figure 10. It is observed that the specific heat capacity is increasing with increase in temperature and matches very well with the reported values[1]. The specific heat capacity values of the samples Y_R, Y_{SM} and Y_{RM} are 0.462, 0.465 and 0.467 $Jg^{-1}K^{-1}$ respectively at 303K where as the values reduces to 0.522, 0.526 and 0.527 $Jg^{-1}K^{-1}$ respectively at 570K.

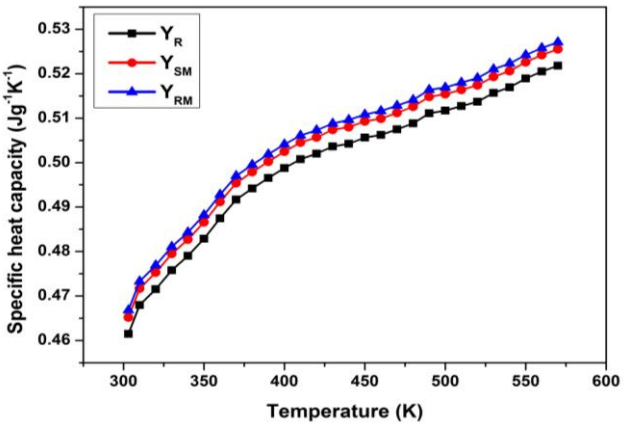

Figure 10: Specific heat capacity of yttria pellets fabricated using different sintering techniques.

I

n addition to the transparent nature an infrared transparent window should protect the highly delicate infrared sensor from the harsh environments of missile flight. The strength and hardness of the polycrystalline ceramics highly dependent on the grain size [48]. Hardness is a measure of resistance to indentation. As grain size decreases the strength and hardness increases [49]. In the present study Vickers indenter method is used for testing the hardness of the sample at room temperature. The apparent hardness is measured from the load and the affected area under indentation made by the diamond indenter. In most of the ceramics the hardness is dependent on the grain size and the load applied. If the hardness of the material decreases with increase in load it is called indentation size effect (ISE)[50].

In the present work to study the effect of load and grain size on the hardness of the sintered pellets different loads 0.98,1.96,2.94 and 4.9 N are applied on the pellets Y_R, Y_{SM} and Y_{RM} respectively. For every load five indentations are made on the surface at different positions from which the average apparent hardness for a particular load is measured. The hardness values obtained for different loads on the pellets sintered via different techniques are shown in figure 11.

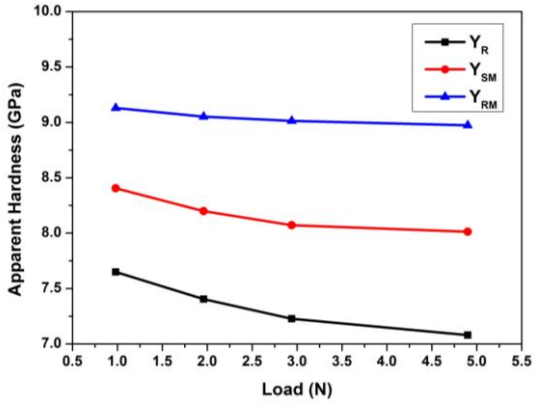

Figure 11 : Variation in apparent hardness with load

The maximum hardness of 9.1GPa is shown by the pellet Y_{RM} for a load of 0.98N. The percentage decrease of hardness with load is minimum in the case of Y_{RM}, whereas the minimum hardness of 7.6 GPa is shown by the pellet Y_R and the percentage decrease in hardness with load is also greater for it. The percentage decrease in hardness with load is 7.34% in the present case where as that for Y_{RM} it is 1.72% . The apparent hardness of pellet Y_{SM} is found to be 8.4 GPA and the percentage decrease in hardness with load is 4.7%.

Mayer's law is generally used to describe the ISE effect by the relation

$$P = A.d^n$$

Where P is the load applied and d is the resultant indent diagonal. A and n are constants. The slope of the graph obtained by plotting ln P along Y axis and log d along X-axis is n and is called as Meyer's index [50]. To find the Meyer's constant a graph is plotted with ln F along Y-axis and ln d along X-axis and is shown in the figure 12. Here P is the applied load in newton and d is the diagonal length of indentation in micrometer.

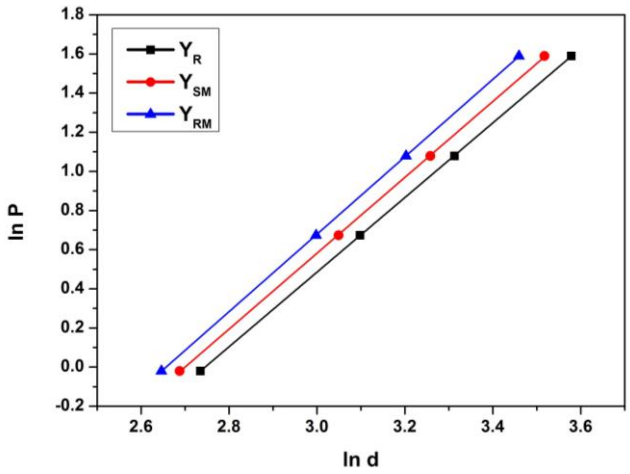

Figure 12 : ln P-ln d graph

The slopes obtained from the linear fit are 1.91, 1.94 and 1.98 for samples Y_R,Y_{SM} and Y_{RM} respectively. All the n values are less than 2, which indicates that all the samples show ISE behaviour. For the load independent hardness the value of n should be 2 [51]. To find the load independent microhardness proportional specimen resistance model(PSR) [52] is used and compared the result with modified PSR (MPSR) model[53]. Based on the PSR model the load P and indentation size d are connected by the relation

$$\frac{P}{d} = a_1 + a_2 d$$

Where a_1 is a constant related to the proportional resistance of the specimen which is directly proportional to the Young's modulus and a_2 is a constant related to load independent micohardness, H_0, and a_1/a_2 is a measure of residual stress connected with the defects in the specimen [52]. A graph $\frac{P}{d}$ versus d is plotted as shown in figure 13 and the slope $\frac{P_c}{d_0^2}$ is obtained for the samples Y_R, Y_{SM} and Y_{RM}. The slope of the graph ie $\frac{P_c}{d_0^2}$ multiplied by Vicker's conversion factor 1.854 will give the load independent microhardness H_0 [54] .The parameters used and the results obtained are tabulate in table 1 . The maximum load independent hardness of 8.85 GPa is obtained for the sample Y_{RM} sintered using resistive coupled microwave sintering. For the samples Y_{SM} and Y_R the hardness obtained are 7.68 and 6.64 GPa respectively which are low compared to that of sample Y_{RM}.

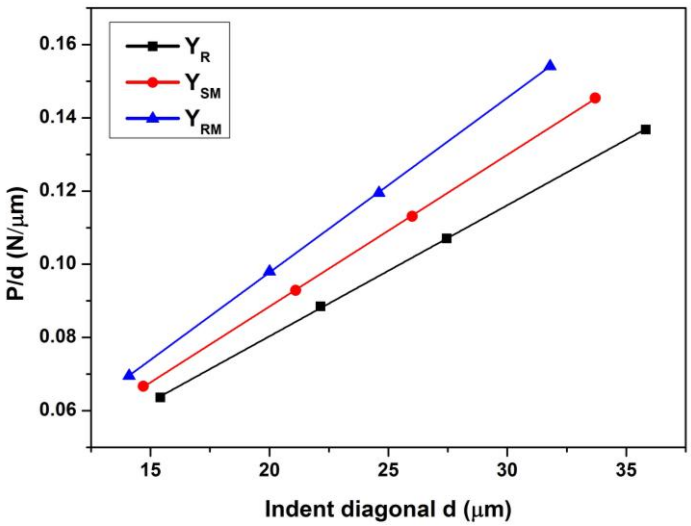

Figure 13: P/d-d graph PSR model

Table 1 : Load independent hardness of yttria pellets sintered by different fabrication methods based on PSR model.

Samples	**a_1 (N/μm)**	$a_2 = \frac{P_c}{d_0^2}$ **(N/μm²)**	H_0 **(GPa)**
Y_R	0.00876	0.00358	6.64
Y_{SM}	0.00558	0.00414	7.68
Y_{RM}	0.00231	0.00477	8.85

But in the literature there are reports that for wide range of loads some materials show non linear nature. So a modified PSR(MPSR) model is also used as a comparison[55]. It is a semi empirical relation connecting the load P and the indentation size d and is given by

$$P = a_0 + a_1 d + a_2 d^2$$

Where P is the applied load, d is the indentation size, a_0, a_1 and a_2 are parameters obtained from curve fitting of the experimental results. The graph connecting indentation load and indent diagonal is plotted and is shown in figure 14. The load independent hardness called true hardness H_T can be obtained from a_2 by the relation $H_T = ka_2$

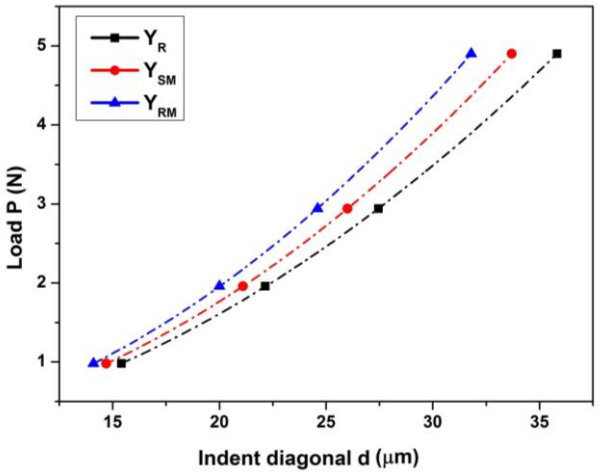

Figure 14: Variation in indentation size with applied load

Where k is a constant equal to 1.8544 for Vicker's indenter and 14.229 for Knoop indenter[53]. A P versus d graph is plotted and the parameters obtained are tabulated in table 2.

Table 2: True hardness of yttria pellets sintered by different fabrication methods based on MPSR model.

Samples	**a_0 (N)**	**a_1 (N/μm)**	$a_2 = \frac{P_c}{d_0^2}$ **(N/μm²)**	H_T **(GPa)**
Y_R	0.05924	0.0162	0.00347	6.44
Y_{SM}	0.0527	0.00676	0.00425	7.88
Y_{RM}	0.00064	0.00227	0.00477	8.85

The hardness calculated for the sample Y_{RM} using the PSR model and MPSR model are found to be the same . So the true hardness ie the load independent hardness for the pellet sintered using resistive coupled microwave sintering is 8.85 GPa. The greater hardness achieved without compromising the transmittance and thermal properties is a remarkable result which may find application in future infrared windows in strategic defence and space missions.

CONCLUSIONS

Phase pure nanostructured yttria (Y_2O_3) powders are synthesised by a single step auto-igniting combustion technique. The XRD result shows that the sample crystallised in body centred cubic structure and have an average particle size of 15nm. A sintering strategy by coupling resistive heating and microwave heating in definite proportion is used to sinter the samples to high density (>99%) without any sintering aids or pressure. In this resistive coupled microwave sintering there is a substantial reduction in sintering temperature and soaking duration. The sintering temperature is reduced by ~90^{o}C compared to that in microwave sintering and by ~170^{o}C compared to that in conventional sintering. The pellet sintered via resistive coupled microwave heating showed reduced grain size, minimum porosity and better hardness compared to the microwave sintered and resistive sintered counter parts. There is a nominal reduction in the thermal conductivity and diffusivity of the pellet sintered using resistive coupled microwave heating compared to the other two pellets but the values are in the ideal range suitable for infrared transparent windows. The pellet sintered using resistive coupled microwave heating shows high load independent hardness of 8.85 GPa and is a remarkable result that it is achieved without compromising the transmittance properties. The hardness corresponding to the pellets sintered using microwave and resistive heating are 7.88 and 5.89 GPa respectively. The results clearly indicate that the yttria ultra fine nanophase powder synthesised using single step combustion method followed by resistive coupled microwave sintering can be used very effectively for the fabrication of improved infrared transparent windows and domes.

ACKNOWLEDGEMENTS

This work is supported by the Department of Science and Technology- Science and Engineering Research Board, Government of India under Grant No. SB/S2/CMP-0021/2013.

REFERENCES

[1] Harris D C, 1999, Materials for Infrared Windows and Domes, Properties and Performance. SPIE Press, Bellingham, WA.

[2] Deborah D S and Aldo R B, 2008, "Industrial developments in the field of optically transparent inorganic materials: A survey of recent patents", Recent Patents on Materials Science 1 , pp. 56-73.

[3] Qin X, Yang H, Shen D, Chen H, Zhou G, Wang S, Luo D, Tang D, Zhang J,and Ma J, 2013 "Fabrication and Optical Properties of Highly Transparent Er:YAG Polycrystalline Ceramics for Eye-Safe Solid-State Lasers", Int. J. Appl. Ceram. Tec.10 (1), pp. 123-128.

[4] Lan Y H , Jun J Z, Jian M X, Wei W S, 2010, "New Development of Transparent Alumina Ceramics", J. Inorg. Mater., 25 (8), pp.795-800.

[5] Grujicic M, Bell W C and Pandurangan B, 2012, "Design and material selection guidelines and strategies for transparent armor systems", Mater Design 34, pp.808–819.

[6] Salem J A, 2013, "Transparent Armor Ceramics as Spacecraft Windows", J.Am.Ceram.Soc. 96(1), pp. 281-289.

[7] Ratches J A, 2011, "Review of current aided/automatic target acquisition technology for military target acquisition tasks", Opt. Eng. 50(7), pp. 720011-720018.

[8] Curtis C E, 1957, " Properties of Yttrium Oxide Ceramics", J.Am.Ceram.Soc. 40(8), pp.274-278.

[9] Serivalsatit K, Kokuoz B, Kokuoz B Y, Kennedy M and Ballato John, 2010, "Synthesis, Processing and Properties of Submicrometer-Grained Highly Transparent Yttria Ceramics", J.Am.Ceram.Soc. 93(5), pp.1320-1325.

[10] Boniecki M, Librant Z, Wesolowski W, Gizowska M, Osuchowski M, Perkowski K, Witek A and Witoslawska, 2016, "The thermal shock resistance of Y_2O_3 ceramics", Ceram. Int. 42, pp. 10215-10219.

[11] Pastor A C and Pastor R C, 1967, " Crystal Growth above 2200^{o}C by the Verneuil Method", Mater.Res.Bull. 2, pp. 555-559.

[12] Tsukuda Y, Properties of blackY_2O_3 sintered bodies,Mater.Res.Bull 16(1981) 453-459.

[13] Sova R M, Linevsky M J, Thomas M E, Mark F F, High-temperature infrared properties of sapphire, AlON, fused silica, yttria, and spinel, Infrared. Phys. Techn. 39 (1998) 251-261.

[14] Harris D C, 1998, "Durable 3-5μm transmitting infrared window materials", Infrared Phys.Techn. 39, pp.185-201.

[15] Krell A , Hutzler T and Klimke J, 2009 , "Transmission physics and consequences for materials selection, manufacturing, and applications", J. Eur. Ceram. Soc. 29, pp.207–221.

[16] Oghbaei M and Mirzaee O, 2010, "Microwave versus conventional sintering : A review of fundamentals, advantages and applications", J.Alloy.Compd. 494, pp.175-189.

[17] Jiang D T, Hulbert D M, Tamburini U A, Ng T, Land D and Mukherjee A K, 2008, "Optically transparent polycrystalline Al_2O_3 produced by spark plasma sintering", J.Am. Ceram. Soc.91(1), pp.151-154.

[18] Apetz R and Bruggen M P B, 2003, " Transparent alumina: a light-scattering model", J.Am.Ceram. Soc.. 86(3), pp. 480-486.

[19] Jiang D T and Mukherjee A K, 2010, "Spark plasma sintering of an infrared transparent Y_2O_3-MgO nanocomposite", J. Am. Ceram. Soc.93(3), pp.769-773.

[20] Moshtanghioun B M, Gracia D G, Rodriguez A D and Todd R I, 2016, "Grain size dependence of hardness and fracture toughness in pure near fully-dense boron carbide ceramics", J. Eur. Ceram. Soc. 36(7), pp. 1829-1834.

[21] Ahmadi B, Reza S R, Vadeqani M A and Barekat, 2016, "Mechanical and optical properties of spark plasma sintered transparent Y_2O_3 ceramics", Ceram. Int. 42(15), pp.17081-17088.

[22] Eilers H, 2007, "Fabrication, optical transmittance, and hardness of IR-transparent ceramics made from nanophase yttria", J. Eur.Ceram. Soc. 27, pp.4711-4717.

[23] An L, Ito A and Goto T, 2012, "Transparent yttria produced by spark plasma sintering at moderate temperature and pressure profiles", J. Eur. Ceram. Soc. 32, pp.1035-1040.

[24] Luo J, Zho Z and Xu J, 2012, "Yttrium oxide transparent ceramics by low-temperature microwave sintering", Mater.res. bull. 47, pp.4283-4285.

[25] Huang Y, Jiang D, Zhang J and Lin Q, 2009, "Fabrication of transparent lanthanum doped yttria ceramics by combination of two-step sintering and vacuum sintering", J. Am. Ceram. Soc. 92(12), pp.2883-2887.

[26] Wang Z, Zhang L, Yang H, Zhang J,Wang L and Zhang Q, 2016, "High optical quality Y_2O_3 transparent ceramics with fine grain size fabricated by low temperature air pre-sintering and post HIP treatment", Ceram. Int. 42, pp.4238-4245.

[27] Yan D, Xu X, Lu H, Wang Y, Liu P and Zhang J, 2016, "Fabrication and properties of Y2O3 transparent ceramic by sintering aid combinations", Ceram.Int., Article in press doi: 10.1016/j.ceramint.2016.07.089.

[28] Ghaderi M, Razavi R S, Estarki M R L and Ghorbanu S, 2016, "Spark plasma sintering of transparent Y2O3 ceramic using hydrothermal synthesized nanopowders", Ceram. Int. 42(13), pp.14403-14410.

[29] Gan L, Park Y J, Zhu L L, Go S, Kim H, Kim J M and Ko J W, 2016, "Enhancement of the optical transmittance of hot-pressed transparent yttria ceramics by a multi-step sintering process", Ceram. Int. 42(12), pp. 13952-13959.

[30] He J, Li X, Liu S, Zhu Q, Li J G and Sun X, 2015, "Effect of pre-treatment of starting powder with sulphuric acid on the fabrication of yttria transparent ceramics", J. Eur. Ceram. Soc. 35, pp. 2369-2377.

[31] Klein C A, 1998, "Thermal shock resistance of infrared transmitting windows and domes", Opt.Eng 37(10), pp.2826-2836.

[32] Gentilman R L, 1986, "Current and emerging materials for 3-5 micron IR transmission", Proc.SPIE, 683, pp.2-11.

[33] J. James, R. Jose, Asha M. John and J. Koshy, 2004, " A Single step process for the synthesis of nanoparticles of ceramic oxide powders"; U.S.Patent 6761866.

[34] Thomas J K, Padma Kumar H, Pazhani R, Solomon S, Jose R and Koshy J , 2007, "Synthesis of strontium zirconate as nanocrystals through a single step combustion process", Mater. Lett. 61, pp.1592–1595.

[35] Thomas J K, Padma Kumar H, Annamma John, Suni V,Joy K, Solomon S and Koshy J, 2009, "Nanocrystalline $GdBa_2HfO_{5.5}$ perovskite dielectric material-A single-step synthesis and its characterisation", J.Phys.Chem.Solids. 70, pp.703-706.

[36] Langford L I and Wilson A J C, 1978, " Scherrer after Sixty Years: A Survey and Some New Results in the Determination of Crystallite Size", J.Appl.Cryst. 11, pp.102-113.

[37] Zuo F, Badev A, Saunier S, Goeuriot D, Heuguet R and Marinel S, 2014, "Microwave versus conventional sintering : Estimate of the apparent activation energy for densification of α-alumina and zinc oxide", J. Eur. Ceram. Soc. 34(12), pp.3103-3110.

[38] Sun H, Zhang Y, Gong H , Li T, Li Q, Microwave sintering and kinetic analysis of Y_2O_3-MgO composites, Ceram. Int. 40 (2014) 10211-10215.

[39] Rybakov K I, Olevsky E A and Krikun E V, 2013, "Microwave sintering: Fundamentals and Modeling", J.Am.Ceram.Soc. 96(4), pp.1003-1020.

[40] Croquesel J, Bouvard D, Chaix J M, Carry C P, Saunier S and Marinel S, 2016, "Direct microwavesintering of pure alumina in a single mode cavity: Grain size and phase transformation effects", Acta Mater. 116, pp.53-62.

[41] Goldstein A, Krell A, 2016, "Transparent ceramics at 50: Progress made and Further Prospects", J.Am.Ceram. Soc.1, pp. 1-25.

[42] Tritt T M, 2004, Thermal Conductivity, Theory, Properties and Applications, Springer, New York, NY.

[43] Parish M, Pascucci M, Corbin N, Puputti B, Chery G and Small J, 2011, " Transparent ceramics for demanding optical applications", Proc.SPIE, 8016, pp.80160B 1-6.

[44] Limarga A M and Clarke D R, 2011, "The grain size and temperature dependence of the thermal conductivity of polycrystalline tetragonal yttria stabilized zirconia", Appl. Phys. Lett. 98, pp.2119061-2119063.

[45] Kingery W D, Fancl J, Coble R L and Vasilos T, 1954, "Thermal Conductivity, X, Data for several pure oxide materials corrected to zero porosity", J. Am. Ceram. Soc., 37[2], pp. 107-110.

[46] Fayette S, Smith D S, Smith A and Martin C, 2000, "Influence of grain size on the thermal conductivity of tin oxide ceramics", J. Eur. Ceram.Soc.20, pp. 297-302.

[47] Troph W J and Harris D C, 1989, "Mechanical thermal and optical properties of yttria and lanthana-doped yttria", Proc.SPIE 1112, pp.9-19.

[48] Callister W D, 2007, Materials Science and Engineering: An Introduction, 7th Edition, Wiley, New York.

[49] Osoro G M, Moya J S and Pecharroman C, 2012, "Transparent alumina by vacuum sintering", J. Eur.Ceram.Soc. 32, pp.2925-2933.

[50] Roy T K, 2015, " Assessing hardness and fracture toughness in sintered zinc oxide ceramics through indentation technique", Mater. Sci. Eng.A 640, pp.267-274.

[51] Sahin O, Uzun O, Lizer M S, Gocmez H and Kolemen U, 2008, " Dynamic hardness and elastic modulus calculation of porous SiAlON ceramics using depth-sensing indentation technique", J. Eur. Ceram. Soc. 28(6), pp. 1235-1242.

[52] Li H and Bradt R C, 1993, "The microhardness indentation load/size effect in rutile and cassiterite single crystals", J. Mater.Sci. 28 (4), pp. 917-926.

[53] Gong J and Li Y, 2000, "An energy-balance analysis for the size effect in low-load hardness testing", J.Mater. Sci. 35, pp.209-213.

[54] Mukerji S and Kar T, Vicker's, 1999, "Microhardness Studies of L-arginine Hydrobromide Monohydrate Crystals (LAHBr)", Cryst. Res. Technol.34(10), pp. 1323-1328.

[55] Gong G, Wu J and Guan Z, 1998, " Load dependence of the apparent hardness of silicon nitride in a wide range of loads", Mater.lett.35(1-2), pp. 58-61.